**Analytical approach leveraging orbital perturbations for spacecraft end-of-life disposal design**

Xiaodong Lu [(1)], Camilla Colombo [(2)]

*(1) Politecnico di Milano*
*Milan, Italy*
*Email: xiaodong.lu@polimi.it*

*(2) Politecnico di Milano*
*Milan, Italy*
*Email: camilla.colombo@polimi.it*

***Abstract* – This paper presents an end-of-life disposal manoeuvres design technique targeting an Earth re-entry, using a triple-averaged model for orbital perturbations. The natural perturbations are enhanced by impulsive manoeuvres which moves a spacecraft into a trajectory evolving naturally to Earth re-entry. The exploitation of the triple-averaged model significantly reduces computational burden of manoeuvre optimisation. The proposed technique is applied to a Highly Elliptical Orbit mission and the results obtained are validated through a high-fidelity model.**

## I. INTRODUCTION

Modern society benefits a lot from services provide by space activities, while these activities have a cost of creating large numbers of space objects. The space object population has been increasing for many years and becoming more rapidly in last decades due to the deployment of mega-constellations. Since the beginning of space era, about 16,990 satellites have been placed into Earth orbit and only about 9000 of them are still functioning. About 35,150 debris objects are regularly tracked by Space Surveillance Networks (SSN) and maintained in their catalogue [1][2] The increasing number of space objects increases probability of collisions between objects leading to a cascade process, known as the Kessler's syndrome [3]. In response to this situation, the Inter-Agency Space Debris Coordination Committee (IADC) published space debris mitigation guidelines specifying different mitigation measures, one of which is to design end-of-life disposal strategies for spacecrafts, preventing prolonged stay in geostationary orbit (GEO) and limiting passage in low Earth orbit (LEO) [4] and is now discussing measures also for the GNSS regions.

Successful end-of-life disposals make large contribution to debris mitigation and remediation. However, implementation of end-of-life disposal could consume large amount of propellant and hence significantly increases the economic cost, which decreases feasibility of disposal strategies and discourages spacecraft operators from implementing disposal strategies and meeting mitigation guidelines. Therefore, end-of-life disposal manoeuvres should be optimised so that least propellant is needed for a successful disposal, this can be achieved if the natural long-term dynamics of natural orbit perturbations is enhanced [5]. On the other hand, one of the most important problems for manoeuvre optimisation is expensive computational cost since long-term numerical orbit propagation is involved. Using semianalytical models in the manoeuvre optimisation could help mitigate this problem, this could also contribute to implementing such computation autonomously on-board since due to the long deorbiting time some corrections may be needed.

This paper develops a triple averaged model for orbital perturbations, averaging disturbing functions over the period of a spacecraft orbit, the period of a third body and the period of right ascension of ascending node. The triple averaged disturbing functions allow one to get a Hamiltonian of one-degree-of-freedom with introducing the famous Kozai parameter. The averaged model is used in manoeuvre optimisation for end-of-life disposal of a spacecraft in a Highly Elliptical Orbit (HEO), which is mainly perturbed by the Earth oblateness and gravitational attractions due to the Moon and the Sun.

The paper is organised as follows. Section II develops the triple averaged model for orbital perturbation and obtain the averaged Hamiltonian. Section III reports the end-of-life disposal strategy design of a HEO spacecraft. Section IV gives a case study of applying the proposed technique to a HEO mission. Finally, Section V concludes the paper and summarizes the main results of the paper.

## II. SEMIANALYTICAL MODELS FOR ORBITAL PERTURBATIONS

The dynamics of a perturbed orbit of a spacecraft is described by the well-known Lagrangian planetary equations [6],

$$
\begin{aligned}
\frac{da}{dt} &= \frac{2}{na}\frac{\partial R}{\partial M} \\
\frac{de}{dt} &= \frac{1-e^2}{na^2 e}\frac{\partial R}{\partial M} - \frac{\sqrt{1-e^2}}{na^2 e}\frac{\partial R}{\partial \omega} \\
\frac{di}{dt} &= \frac{1}{na^2\sqrt{1-e^2}\sin i}\left(\cos i\frac{\partial R}{\partial \omega} - \frac{\partial R}{\partial \Omega}\right) \\
\frac{d\Omega}{dt} &= \frac{1}{na^2\sqrt{1-e^2}\sin i}\frac{\partial R}{\partial i} \\
\frac{d\omega}{dt} &= \frac{\sqrt{1-e^2}}{na^2 e}\frac{\partial R}{\partial e} - \cos i\frac{d\Omega}{dt} \\
\frac{dM}{dt} &= n - \frac{1-e^2}{na^2 e}\frac{\partial R}{\partial e} - \frac{2}{na}\frac{\partial R}{\partial a}
\end{aligned} \tag{1}
$$

where $a, e, i, \Omega, \omega, M$ are classical Keplerian elements, $n = \sqrt{\mu/a^3}$ in which $\mu$ is the gravitational parameter of the Earth, and $R$ is a disturbing function depending on the perturbations of interest.

The orbit of a spacecraft in HEO is mainly affected by the Earth's oblateness, and lunisolar perturbations. The disturbing function of perturbation due to the Earth's oblateness is given by [7]:

$$R_{J_2} = -\frac{\mu}{r}J_2\left(\frac{R_\oplus}{r}\right)^2\frac{1}{2}(3\sin^2(\omega+f)\sin^2 i - 1), \tag{2}$$

where $J_2$ is the second zonal harmonics, $R_\oplus$ is the equatorial radius of the Earth, and $r$ is the radial distance between a spacecraft and the Earth given by

$$r = \frac{a(1-e^2)}{1+e\cos f}, \tag{3}$$

where $f$ is true anomaly of a spacecraft.

The disturbing function of third-body perturbation is given by:

$$R_{3b} = \frac{\mu_3}{r_3}\sum_{l=2}^{\infty}\left(\frac{r}{r_3}\right)^l P_l(\cos S), \tag{4}$$

where $\mu_3, r_3$ is the gravitational parameter of the third body and the radial distance between the third body and the Earth, respectively, $P_l(\cdot)$ is the $l$-th order Legendre polynomial and $S$ is the angle between the position vector of a spacecraft and the one of a third body, which is given by [8]

$$
\begin{aligned}
\cos S = \hat{\mathbf{r}}\cdot\hat{\mathbf{r}}_3 &= (\hat{\mathbf{p}}\cos f + \hat{\mathbf{q}}\sin f)\cdot\hat{\mathbf{r}}_3 \\
&= A\cos f + B\sin f,
\end{aligned} \tag{5}
$$

where $\hat{\mathbf{r}}, \hat{\mathbf{r}}_3$ represent the directions of a spacecraft and a third body, respectively, $\hat{\mathbf{p}}$ is the unit vector pointing the perigee and $\hat{\mathbf{q}}$ is orthogonal to $\hat{\mathbf{p}}$ in the orbital plane.

The partial derivatives of a disturbing function with respect to Keplerian elements can be computed and the evolution of a spacecraft orbit can hence be obtained by numerically integrating (1). However, numerical integration leads to slow computation, especially when the dynamics is included in the context of manoeuvre optimisation or trajectory design process. On the other hand, only long periodic and secular variations are of interest in many applications.

The semianalytical models based on averaging techniques can tackle this problem. The idea is to average the disturbing function over fast angles, to eliminate the short periodic terms in the disturbing function.

The disturbing function of the $J_2$ perturbation is averaged over one orbital period of a spacecraft [6],

$$\overline{R}_{J_2} = \frac{\mu J_2 R_\oplus^2}{4a^3\eta^3}(2 - 3\sin^2 i), \tag{6}$$

where $\eta = \sqrt{1-e^2}$ is defined for convenience of computation. In the same manner, the disturbing function of third-body perturbation [7] is averaged as

$$\overline{R}_{3b} = \frac{\mu_3}{r_3}\sum_{l=2}^{\infty}\left(\frac{a}{r_3}\right)^l F_l(A,B,e), \tag{7}$$

and averaged again over one orbital period of the perturbing body,

$$\overline{\overline{R}}_{3b} = \frac{\mu_3}{a_3}\sum_{l=2}^{\infty}\left(\frac{a}{a_3}\right)^l F_l(\alpha_A,\beta_A,\alpha_B,\beta_B,e), \tag{8}$$

where $\alpha_A, \beta_A, \alpha_B, \beta_B$ are defined as

$$\alpha_A = \hat{\mathbf{p}}\cdot\hat{\mathbf{p}}_3, \beta_A = \hat{\mathbf{p}}\cdot\hat{\mathbf{q}}_3, \alpha_B = \hat{\mathbf{q}}\cdot\hat{\mathbf{p}}_3, \beta_A = \hat{\mathbf{q}}\cdot\hat{\mathbf{q}}_3,$$

in which $\hat{\mathbf{p}}_3, \hat{\mathbf{q}}_3$ are defined in the same manner as $\hat{\mathbf{p}}, \hat{\mathbf{q}}$.

The total single- and double-averaged disturbing functions are following,

$$\overline{R} = \overline{R}_{J_2} + \overline{R}_{Sun} + \overline{R}_{Moon}, \tag{9}$$

$$\overline{\overline{R}} = \overline{R}_{J_2} + \overline{\overline{R}}_{Sun} + \overline{\overline{R}}_{Moon}. \tag{10}$$

To further simplify the dynamics model, one can average the third body disturbing function over period of variation of $\Omega$, also known as elimination of the node,

$$\overline{\overline{\overline{R}}}_{3b} = \frac{\mu_3}{a_3}\sum_{l=2}^{\infty}\left(\frac{a}{a_3}\right)^l F_l(e,i,\omega,e_3,i_3,\omega_3), \tag{11}$$

where the node of the third body's orbit $\Omega_3$ is also eliminated since it is coupled with node of a spacecraft orbit.

The averaging technique allows one to eliminate fast angles in the disturbing function, hence separating long-periodic and secular effects from the short-periodic ones. This procedure is of importance since it simplifies the manoeuvre optimisation process a lot. The simplified model is validated by comparing with the high-fidelity model obtained by propagating Gauss' planetary equation.

Fig 1 shows that the single- and double-averaged model (orange and yellow lines) coincide well with the high-fidelity model (blue line), while the triple-averaged model (purple line) shows considerable large discrepancies with the results obtained from other models. This is due to the complexity of dynamics of the Earth-Moon-Sun system, that the Moon's orbit is about 5.145 degrees inclined with respect to the ecliptic and the ecliptic has an obliquity of about 23.45 degrees [9].

Nevertheless, the simplification by elimination of the node offers advantage of less computational resources and can be used for preliminary analysis as will be discussed in the following section.

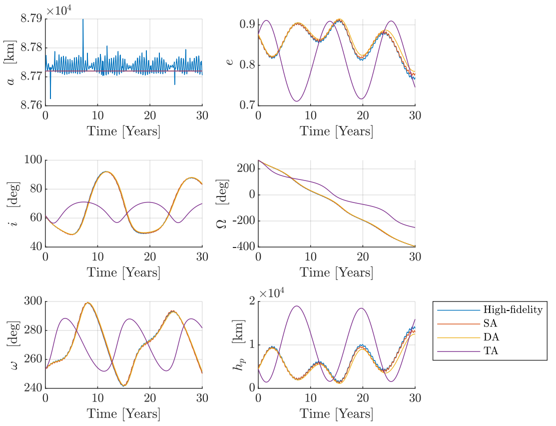

Fig 1. Orbit evolution using averaged and high-fidelity models, High-fidelity: high-fidelity model using Gauss' equations, SA: single averaged model, DA: double averaged model, TA: triple averaged model.

The Hamiltonian formulation of a system allows to understand the behaviours and qualitative insights of dynamics, especially in the long-term evolution. The Hamiltonian of a perturbed two-body system consists of the Hamiltonian of a two-body system and disturbing potentials, which are the negative of corresponding disturbing functions. The Hamiltonian of an orbit around the Earth and perturbed by $J_2$ and lunisolar perturbations is defined as

$$H = -\frac{\mu}{2a} - R_{J_2} - R_{Moon} - R_{Sun}. \quad (12)$$

In the application of end-of-life disposal manoeuvre design, the terms in the Hamiltonian corresponding to short-periodic effects could be removed through abovementioned averaging procedures as only the secular and long-periodic effects of perturbations are of interest. The double-averaged Hamiltonian is retrieved as

$$\bar{\bar{H}} = -\frac{\mu}{2a} - \bar{R}_{J_2} - \bar{\bar{R}}_{Moon} - \bar{\bar{R}}_{Sun}$$
$$= \bar{\bar{H}}\big(a, e, i, \Omega, \omega, i_{Moon}(t), \Omega_{Moon}(t), \omega_{Moon}(t)\big). \quad (13)$$

Here semimajor axis $a_{Moon}$ and eccentricity $e_{Moon}$ of the Moon's orbit is regarded as constants, while $i_{Moon}(t), \Omega_{Moon}(t), \omega_{Moon}(t)$ are time dependent. The Keplerian elements of the Sun are regarded as constants too except for the mean anomaly which is already averaged out.

Thanks to further simplification of elimination of the node, the Hamiltonian can be reduced to a form of $\bar{\bar{\bar{H}}}\big(e, i, \omega, i_{Moon}(t), \omega_{Moon}(t)\big)$, and after dropping the time dependent terms, one could get a Hamiltonian only depending on eccentricity, inclination, and argument of perigee of a spacecraft orbit, $H(e, i, \omega)$. Note that both $J_2$ and lunisolar perturbations do not affect semimajor axis of a spacecraft orbit in the long term.

Furthermore, the so-called Kozai parameter $\Theta = (1 - e^2)\cos^2 i$ is a constant [10] since the $z$-component of angular momentum is conserved. Hence, one can get a Hamiltonian of one degree-of-freedom $H(e, \omega)$ and phase space maps of dynamics. The phase space maps are of importance to both analysis of dynamics and validation of optimal manoeuvres obtained from disposal design process.

As an example, Fig 2 shows the phase space portrait of orbits with a semimajor same as the INTEGRAL mission [11] and the position of the INTEGRAL mission in the phase space using red curve, considering lunar perturbation only. It shows that spacecraft orbits evolve in a libration manner and the maximum and minimum eccentricities are attained when $\omega = \pi/2$. It could be identified that natural evolution of orbits can be enhanced by impulsive manoeuvres at certain points of a phase curve, and the post-manoeuvre orbits evolve at a different phase curve under natural perturbations and reach re-entry conditions by entering the critical region after curtain time.

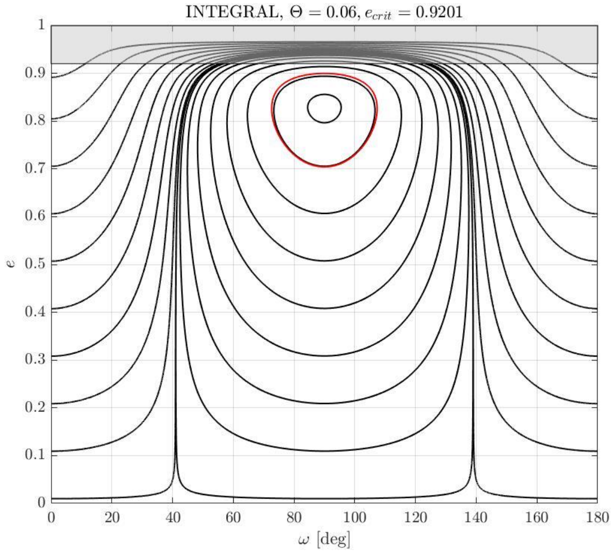

Fig 2. Phase space portrait of the INTEGRAL mission, red: initial phase curve of the INTEGRAL mission, grey zone: critical eccentricity.

## III. DISPOSAL MANOEUVRES DESIGN

The framework described in the previous section is now applied to the design of the end-of-life disposal for a spacecraft targeting an Earth re-entry, particularly a spacecraft in HEO. The re-entry condition of a spacecraft is defined through the minimum perigee height that the spacecraft can reach. A re-entry is deemed as successful if the minimum perigee height is lower than the atmospheric interface of the Earth, that is,

$$h_{p,min} = \min h_p(t) < h_{p,target}, \quad (14)$$

where perigee height is retrieved by Keplerian elements,

$$h_p = a(1 - e) - R_{\oplus}. \quad (15)$$

As semimajor axis of an orbit is not affected secularly by $J_2$ and lunisolar perturbation, the value of perigee height depends only on eccentricity,

$$h_{p,min} = a(1 - e_{max}) - R_{\oplus}, \quad (16)$$

and hence the re-entry condition is translated as

$$e_{max} > e_{crit}, \tag{17}$$

where $e_{crit}$ is the critical eccentricity defined as

$$e_{crit} = 1 - \frac{h_{p,target} + R_{\oplus}}{a}. \tag{18}$$

The natural orbital evolution under the influence of the Earth's oblateness and lunisolar perturbations is enhanced by impulsive manoeuvres. The manoeuvre is modelled as [12][13]

$$\Delta \mathbf{v} = \begin{bmatrix} \Delta v_T \\ \Delta v_N \\ \Delta v_H \end{bmatrix} = \Delta v \begin{bmatrix} \cos\alpha\cos\beta \\ \sin\alpha\cos\beta \\ \sin\beta \end{bmatrix}, \tag{19}$$

in the $(T, N, H)$ reference frame where $T$ axis is tangential to the orbit and always points to the velocity vector, the $N$ axis lies in the orbital plane, normal to the velocity vector, and the $H$ axis is normal to the orbital plane. The variation of Keplerian elements $\Delta kep$ after an impulsive manoeuvre at time $t_m$ can be obtained by Gauss' variational equations [14], which is following,

$$\begin{aligned}
\Delta a &= \frac{2}{n\sqrt{1-e^2}}\sqrt{1+2e\cos f_m + e^2}\,\Delta v_T \\
\Delta e &= \frac{\sqrt{1-e^2}}{na\sqrt{1+2e\cos f_m + e^2}} \\
&\quad \left[2(\cos f_m + e)\Delta v_T - \sqrt{1-e^2}\sin E_m\,\Delta v_N\right] \\
\Delta i &= \frac{r\cos u}{na^2\sqrt{1-e^2}}\Delta v_H \\
\Delta \Omega &= \frac{r\sin u}{na^2\sqrt{1-e^2}\sin i}\Delta v_H \\
\Delta \omega &= \frac{\sqrt{1-e^2}}{nae\sqrt{1+2e\cos f_m + e^2}} \\
&\quad [2\sin f_m\,\Delta v_T + (\cos E_m + e)\Delta v_N] - \cos i\,\Delta\Omega \\
\Delta M &= n - \frac{1-e^2}{nae\sqrt{1+2e\cos f_m + e^2}} \\
&\quad \left[\left(2\sin f_m + \frac{2e^2}{\sqrt{1-e^2}}\sin E_m\right)\Delta v_T \atop +(\cos E_m - e)\Delta v_N\right]
\end{aligned} \tag{20}$$

where $f_m$ is the true anomaly where the manoeuvre is applied, $E_m$ is given following,

$$tan\frac{E_m}{2} = \sqrt{\frac{1-e}{1+e}}\,tan\frac{f_m}{2}, \tag{21}$$

and $u = \omega + f_m$.

The Keplerian elements after manoeuvre could be obtained through

$$kep_{post} = kep_{pre} + \Delta kep, \tag{22}$$

and hence the triply averaged Hamiltonian of dynamics is computed. The new elements define a trajectory in the new phase space after the manoeuvre, corresponding to the new Hamiltonian $H(e, \omega)$. The maximum and minimum eccentricity condition is $\omega = \pi/2$, then finding the maximum eccentricity is a problem of solving a nonlinear equation $H(e_{max}, \pi/2) = H(e_{post}, \omega_{post})$, for which various tools are available. The re-entry is deemed successful if (17) is satisfied.

The greatest advantage of using triple averaged Hamiltonian to obtain the maximum eccentricity and hence the minimum perigee height is that it transfers a constraint of differential equations to a constraint of a nonlinear equation, which avoid the heavy computation due to numerical orbit propagation.

The cost function of optimisation is defined by a weighted sum of the terminal error and $\Delta v$ as

$$J = \max\left(\frac{h_{p,min} - h_{p,target}}{h_{p,target}}, 0\right) + w\Delta v, \tag{23}$$

where $w$ is a user-defined weight based on mission scenarios.

## IV. CASE STUDY

As a case study, this paper computes the possible disposal manoeuvres for a HEO mission. The Keplerian elements of spacecraft at 12:00 on 22/03/2013 is given as initial conditions.

Table 1. Initial orbital elements at 12:00 on 22/03/2013

| $a$ [km] | $e$ | $i$ [deg] | $\Omega$ [deg] | $\omega$ [deg] | $M$ [deg] |
|---|---|---|---|---|---|
| 87720 | 0.8766 | 61.8 | 266.4 | 253.2 | 188.3 |

The time interval for disposal design is set from the initial time to 01/01/2023, and whole interval is divided into 40 points evenly as initial conditions for manoeuvre optimisation. The target perigee height for re-entry is set as 120 km and the weight in the cost function is set as 0.01.

The required magnitudes of $\Delta v$ between 22/03/2013 and 01/01/2023 are shown in Fig 3. It could be identified that there are two periods, from 2015 to mid-2016, and from 2019 to 2020, when no manoeuvre is needed to reach the re-entry condition, while there are other two periods, from initial time to 2014, and from 2022 to 2023, the required $\Delta v$ reaches our limit for the manoeuvre magnitude. Fig 4 shows the directions of manoeuvres performed in terms of in-plane and out-of-plane angles $\alpha, \beta$. It is shown that most manoeuvres stay in the $TN$ plane, since most values of the angle $\beta$ are near 0, and that most manoeuvres are close to the tangential direction or the opposite of tangential direction, since most values of the angle $\alpha$ are near 0, 180, and 360 degrees.

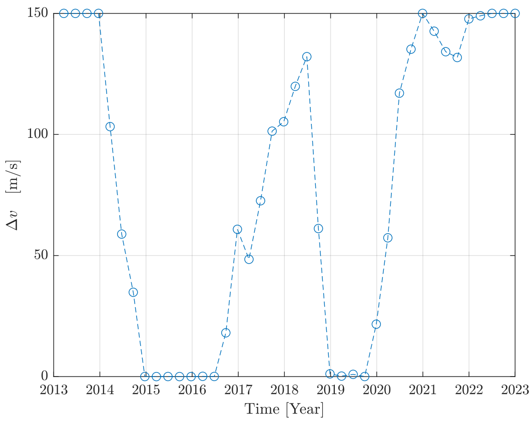


Fig 3. Disposal manoeuvres of a HEO mission

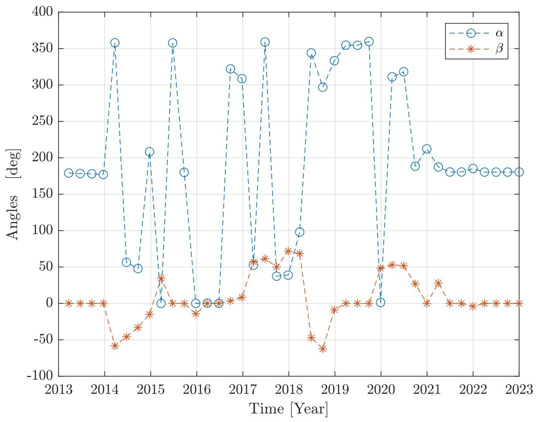


Fig 4. In-plane and out-of-plane angles for manoeuvres

To validate the results of optimisation, the manoeuvres are substituted into double averaged dynamics to propagate the orbits as in Fig 5. It is shown that for one solution the re-entry can be performed in 2020 and for other solutions the re-entries can be performed in 2028. Some solutions do not lead to successful re-entries, which may be due to the low accuracy of the triple averaged model. Nevertheless, the propagation shows that using the proposed technique disposal manoeuvres are successfully computed with a considerably short computational time. The results obtained here serve as a preliminary investigation and could be used as a first guess for refinement of the solution by optimisation using double averaged model or high-fidelity models.

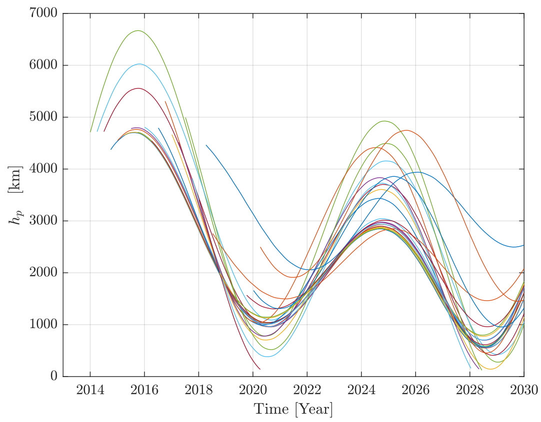


Fig. 5 Validation of the optimisation results

## V. CONCLUSION

This paper proposed a disposal manoeuvre design technique targeting an Earth re-entry based on semi-analytical models for orbital perturbations, in which disturbing functions and hence the Hamiltonian are averaged three times over one period of a spacecraft orbit, one period of a third body, and one period of variation of right ascension of the ascending node. The triple averaged model has a discrepancy compared with the double averaged model and the high-fidelity ones, due to the complexity of the Earth-Moon-Sun system. Nevertheless, the triple averaged model simplifies the manoeuvre optimisation process by transforming a constraint of ordinary differential equations to a constraint of nonlinear algebraic equation, which considerably reduces the computational burden of manoeuvre optimisation process.
The proposed technique is applied to a HEO mission, as a case study. The disposal manoeuvres are computed using triple averaged Hamiltonian, considering a time window from 22/03/2013 to 01/01/2023, and are validated through propagating by a double averaged model. The results shows that the proposed technique is effective in computing the disposal manoeuvres with much less computational time compared to the method using double averaged model. Although the model has relatively less accuracy, the results obtained from the triple averaged model could still be used as a preliminary investigation and first guess for optimisation using the more accurate double averaged model or high-fidelity models to refine the solution.

## VI. ACKNOWLEDGEMENTS

X. Lu acknowledges the funding received from the China Scholarship Council (CSC). The authors acknowledge the support by the European Research Council (ERC) under the European Union’s Horizon 2020 research and innovation program (grant agreement No. 679086 – COMPASS).

## VII. References


[1] ESA, Space Debris by the Numbers. https://www.esa.int/Space_Safety/Space_Debris/Space_debris_by_the_numbers

[2] ESA Space Debris Office, *ESA's Annual Space Environment Report*, 2023. https://www.sdo.esoc.esa.int/environment_report/Space_Environment_Report_latest.pdf

[3] Kessler, D. J., Cour-Palais, B. G., Collision Frequency of Artificial Satellites: the Creation of a Debris Belt, *Journal of Geophysical Research*, Vol. 83, No. A6, 1978, pp. 2637-2646.

[4] IADC, *IADC Space Debris Mitigation Guidelines*, IADC-02-01, Revision 3, 2021. https://iadc-home.org/documents_public/file_down/id/5249

[5] Colombo, C., Long-Term Evolution of Highly-Elliptical Orbits: Luni-Solar Perturbation Effects for Stability and Re-entry, *Frontiers in Astronomy and Space Sciences*, Vol. 6, 2019.

[6] Vallado, D.A., *Fundamentals of Astrodynamics and applications*, Fourth Edition, Microcosm Press, 2013.

[7] Battin, R.H., *An Introduction to the Mathematics and Methods of Astrodynamics*, Revised Edition, AIAA, 1999.

[8] Murray, C.D., Dermott, S.F., *Solar System Dynamics*, Cambridge University Press, 1999.

[9] Gkolias, I., Lara, M., Colombo, C., An ecliptic perspective for analytical satellite theories. *Advances in the Astronautical Sciences*, 2018, 167: 337-351.

[10] Kozai Y., Secular Perturbations of Asteroids with High Inclination and Eccentricity, *The Astronomical Journal*, Vol. 67, No. 9, Nov. 1962, pp. 591-598.

[11] Eismont N. A., Ditrikh A. V., Janin G., Karrask V. K., Clausen K., Medvedchikov A. I., Kulik S. V., Vtorushin N. A., Yakushin N. I., "Orbit design for launching INTEGRAL on the Proton/Block-DM launcher", *Astronomy and Astrophysics*, Vol. 411, N. 1, pp. L37–L41, Nov. 2003, doi:10.1051/0004-6361:20031452

[12] Colombo, C., Letizia, F., Alessi, E. M., Landgraf, M., End-of-life Earth re-entry for highly elliptical orbits: the INTEGRAL mission. In The *24th AAS/AIAA space flight mechanics meeting*, 2014: 26-30.

[13] Lu, X., Colombo, C., Reachable domain analysis for analytical design of end-of-life disposal, in: New Frontiers of Celestial Mechanics: theory and applications, Padova, Italy, 2023.

[14] Colombo C., *Optimal trajectory design for interception and deflection of Near Earth Objects*, Ph.D. Thesis, University of Glasgow, 2010